AUT Journal of Mechanical Engineering

AUT J. Mech. Eng., 5(3) (2021) 465-476
DOI: 10.22060/ajme.2020.18606.5906

Numerical investigation of cardiac function parameters in left heart hemodynamics with stenosed mitral

M. Saidi [1*], R. Samian[2]

[1] Mechanical Engineering Department, Razi University, Kermanshah, Iran
[2]Energy Research Center, Amirkabir University of Technology, Tehran, Iran

ABSTRACT: This work studies the effect of cardiac function parameters on ventricular flow pattern in a stenosed mitral. A three-dimensional simulation is performed employing dynamic mesh based on a geometry and valve flow rates extracted from medical images. Different mitral areas from 6 to 2 cm^2 then different parameters for stenosed 2 cm^2 case are investigated. Special attention has been drawn to compare wall shear stress, blood velocity and pressure distribution, while the power used by ventricle and atrium to pump the blood are also highlighted. Computing the power used by the heart walls to move the blood shows that the stenosed mitral increases the needed force and the energy for the blood flow suction during the early diastole (from 0.06 W for mitral area of 6 cm^2 to 1.28 W for mitral area of 2 cm^2). For the stenosed mitral area of 2 cm2, in the systole, decreasing the ejection fraction to half decreased the maximum ventricle power to around half. In the diastole, decreasing the E/A which is the ratio of early diastole (E wave) and late diastole (A wave) ratio from 4.8 to 1 decreased the maximum ventricle power to one-third. The numerical results confirmed that the compensation mechanism to afford the pumping power could be changing the E/A ratio which leads to enlarged atrium.

Review History:

Received: Jul. 16, 2020
Revised: Aug. 30, 2020
Accepted: Oct. 25, 2020
Available Online: Nov. 12, 2020

Keywords:

Computational fluid dynamics
Dynamic Mesh
E/A ratio
Left Heart
Mitral Stenosis

1- Introduction

The mitral valve (MV) is one of the four valves which guarantees proper control of blood flow through the heart. The MV area varies between 4 and 6 cm^2 in a normal condition [1]. Heart valve diseases could be classified as congenital and acquired. These diseases cause defects in the functionalities of the valve by blood regurgitation, or stenosis and reduction of the valve effective opening area [2]. The spectrum of congenital mitral stenosis (MS) consists of defects including obstruction of left ventricular inflow [3]. MS is a heart valve disease in which narrowing the mitral orifice restricts the blood flow from LA to LV and consequently increases the pressure gradient between the left chambers during the diastole. Rheumatic heart disease (RHD) is the most probable reason for MS worldwide and is more widespread in the developing countries [4]. Moreover, there are some cases in that surgeries may lead to MS.

When the MV becomes diseased, the resultant MV regurgitation is normally fixed surgically [5]. For instance, there are some cases in which MV treatment is performed using MV area reduction which includes restrictive mitral annuloplasty (RMA) and percutaneous edge-to-edge MV repair using a mitral clip [6]. Both treatments result in MV area reduction and therefore could alter the ventricular flow patterns. In addition, Chan et al. [7] showed that MS could take place in patients after MV repair for degenerative mitral regurgitation. Goldstein et al. [8] discussed that RMA could lead to a functional MS which is related to a high degree of recurrent mitral regurgitation. To evaluate and diagnose the MS effect, it is necessary to study heart hemodynamics. Computational fluid dynamics (CFD) by evaluating intra-ventricular flow could be used in this way [9].

Votta et al. [10] reviewed computational methods for patient-specific simulations of native and prosthetic heart valves. Esfahani et al. [11] developed a 2D model to extract the hemodynamic of blood flow in mitral regurgitation during systole by moving arbitrary Lagrange-Euler mesh. They showed that pressure and velocity proportional to the mitral regurgitation. Su et al. [12] assumed tubular and generic atriums and found that proper modeling of atrial flow is necessary. Nevertheless, most numerical studies are limited to LV simulation without considering the atrial model effect on downstream ventricular flow. For instance, recently Meschini et al. [13] studied the stenosis in ventricular flow alteration in presence of MV with different severity levels. The other limitation in numerical studies is assuming the ventricle inflow and outflow as input boundary conditions while mitral stenosis could modify these flows, especially in ventricle inlet. Meschini et al. [14] also studied heart rate effects on the LV hemodynamics with a mono-size MV. They considered heart rates (HR) of 40 to 140 beats per minute (bpm) with constant ejection fraction (EF) of 60% and found that lower flow rates produce a weaker mitral jet with a lower blood kinetic energy

*Corresponding author's email: msaidi@razi.ac.ir

and smaller wall shear stresses. It is expected that considering constant EF leads to higher jet velocity in increased HR. While heart is a muscular system changing HR affects the EF, it worth studying this effect.

The other issue in the present study is the investigation of MV area effect on the left heart flow field and pressure distribution. In addition, the data of relations between valvular properties and cardiac performance are restricted in the literature. In the present study, the effect of MV stenosis is investigated in viewpoint of flow pattern and LV indices. Since the atrium has important role in MV function it has been simulated in the current study. Five different MV areas are selected with the same atrium and ventricle wall motions. Vectors of blood velocity to show the flow feature in different cases in addition to contours to compare the order of velocity magnitude in the LV and wall shear stress contours are among the results compared in the studied cases. Considering the lowest MV area, decreased heart stroke volumes in addition to double the HR have been studied. Also, the E/A ratio has been changed to show the capability of heart to pump the needed blood volume with reasonable power.

2- Materials and Methods

2- 1- Governing Equations

Domain boundaries movement can be simulated using dynamic meshes where mesh nodes are set to new locations. To apply this technique, all of the governing conservation equations should be revised with respect to the velocity of the grid boundaries (v_s) The integral form of the conservation equations of mass and momentum for incompressible flow discretized by finite volume method in the arbitrary Lagrange–Euler (ALE) formulation on an arbitrary control volume V with moving S boundary can be written as [15]

$$\frac{\partial}{\partial t}\int_V \rho dV + \int_S \rho(\mathbf{v}-\mathbf{v}_S).ndS = 0 \tag{1}$$

$$\frac{\partial}{\partial t}\int_V \rho dV + \int_S \rho(\mathbf{v}-\mathbf{v}_S).ndS = 0 \tag{2}$$

where t is the time, ρ is the fluid density, v is the fluid velocity vector in fixed coordinate system, v_s is the velocity vector of the boundary S of the control volume V, n is the normal outward unity vector of this boundary, p is the pressure, and I is the unit tensor. The viscous stress tensor τ can be written as

$$\tau_{ij} = \mu_{eff}\left(\frac{\partial u_i}{\partial x_j} + \frac{\partial u_j}{\partial x_i}\right) \tag{3}$$

where μ_{eff} is summation of μ and μ_t as blood dynamic viscosity and subgrid-scale eddy viscosity, respectively. The blood flowing in the heart chambers can be considered homogeneous Newtonian fluid [16]. The density and dynamic viscosity are assumed constant equal to 1040 kg/m3 and 0.00416 Pa.s, respectively. In the present work, the large eddy simulation (LES) approach is used to consider turbulence. The subgrid-scale stresses resulting from the filtering operation are unknown and require modeling. The subgrid scales (SGS) are modeled using wall-adapting local eddy-viscosity (WALE) model. In this model, the eddy viscosity is modeled by [17]

$$\mu_t = \rho L_S^2 \frac{\left(S_{ij}^d S_{ij}^d\right)^{3/2}}{\left(\bar{S}_{ij}\bar{S}_{ij}\right)^{5/2} + \left(S_{ij}^d S_{ij}^d\right)^{5/4}} \tag{4}$$

where L_S and S_{ij}^d are defined, respectively, as

$$L_S = min\left(kd, C_w V^{1/3}\right) \tag{5}$$

$$S_{ij}^d = \frac{1}{2}\left(\bar{g}_{ij}^2 + \bar{g}_{ji}^2\right) - \frac{1}{3}\delta_{ij}\bar{g}_{kk}^2\bar{g}_{ij}^2 = \frac{\partial \bar{u}_i}{\partial x_j} \tag{6}$$

In this simulation C_w is 0.325 which yields satisfactory results for a wide range of flow [18].

2- 2- Correlating Cardiac Cycle

The methods used to find the heart movements requires spatial and temporal resolution, 4D-Echo (three-dimensional and time-space) provides high-speed resolution, which is especially useful when resolving the fast movements of structures, however, its low spatial resolution and image quality make it difficult to use. On the other hand, methods such as CMR (Cardiac magnetic resonance imaging) and CT (X-ray computed tomography) of the heart provide excellent spatial resolution, but their time resolution is orders-of-magnitude lower than the necessary temporal resolution for the flow simulation so proper interpolation procedures for creating the CFD ready model is required for the simulation of heart movement. This stage of the model is very difficult, and it is still an important challenge in the modeling of the patient's heart [19].

In the present study, an interpolation method is employed for the simulation of heart movement. In this way, only the initial and final stages of heart cycle are considered and interval movement is obtained by considering blood flow in heart valves. Since that blood flow is incompressible heart chambers volumes are related to valve flows. The volume of LV and LA can be written as follows:

$$V_a(t) = V_{a,d} + \int_0^t Q_{inlet}dt - \int_0^t Q_{mitral}dt, \tag{7}$$

$$V_v(t) = V_{v,d} + \int_0^t Q_{mitral}\,dt - \int_0^t Q_{Aorta}\,dt, \tag{8}$$

where subscripts "v" and "a" denote to ventricle and atrium, respectively, $V_v(t)$ represents the volume of ventricle, $V_{v,d}$ is the end diastolic volume of ventricle, $V_{a,d}$ is the end diastolic volume of atrium, Q_{mitral} is the volumetric flow rate passing through MV from atrium to ventricle, Q_{Aorta} is the aortic flow rate which is pumped by LV to aorta, and Q_{inlet} is volumetric flow rate entering LA. The blood flow obtained from the work of Chnafa et al. [20] includes Q_{inlet}, Q_{mitral} and Q_{Aorta} which are total heart inflow, mitral valve flow and aortic valve flow, respectively. By integration of volume flow rate differences and normalizing of ventricle and atrium volume changes, the volumes changes are obtained. Then for the simulation of volumes movement, each heart period is composed of some expansions and contractions and each of these motions is interpolated using a cosine form formulation to find the volume based on discretized volumes in each time data.

$$v(t) = \frac{(v_n + v_{n+1})}{2} + \frac{(v_n - v_{n+1})}{2}\cos\left(\frac{t - t_n}{t_{n+1} - t_n}\pi\right), \quad t_n < t < t_{n+1} \tag{9}$$

Since the movement of heart valves causes difficulty in simulation, a region around these valves is stationary and only heart cavities walls move with the mentioned formulation. Each point on the heart wall fluctuates between end-diastolic and end-systolic volumes by a linear relation between wall movement and volume changes. The end-systolic ventricle points are assumed to locate on a semi-conical shape. More details of the numerical setting and verification of results can be found in previously published work [21].

2- 3- Numerical Settings and Geometry

The blood density of 1040 kg/m^3 and the dynamic viscosity of 0.00416 Pa.s are assumed. The blood flowing in the heart chambers can be considered as a homogeneous Newtonian fluid [16]. The re-meshing and smoothing techniques are employed to simulate the motion of the boundaries considering the volumes of chambers from Chnafa et al. [20] medical images. The time step size of 0.001 s has been used for simulations employing a system with a Core i7-4960X CPU and 32GB RAM.

The schematic of the left heart including ventricle, atrium, aortic valve, and studied mitral areas is depicted in Fig. 1. Five different configurations of the MV with a variable effective area from 2 to 6 cm^2 are shown. The domain discretization is in the order of three million tetrahedral grids, which has been shown by Chnafa et al. [20] that gives mesh independent results for macroscopic parameters. The instantaneous velocity along a line from apex to mitral centerline in addition to average ventricle wall shear stress at t/T=0.5 for different mesh numbers shows that the chosen grid is acceptable, as depicted in Fig. 2.

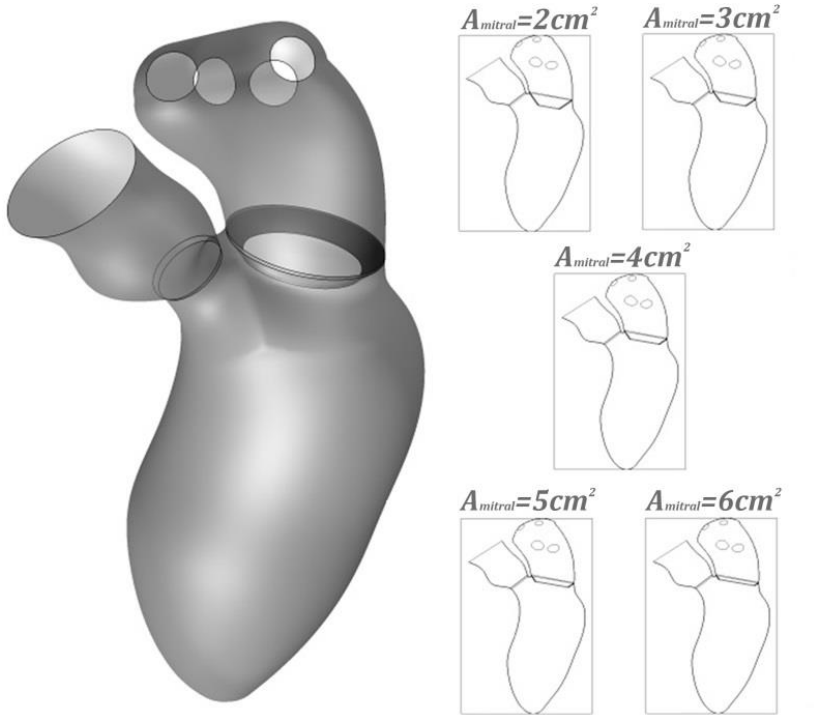

Fig. 1 The left heart geometry with the mitral area from 2 to 6 cm2

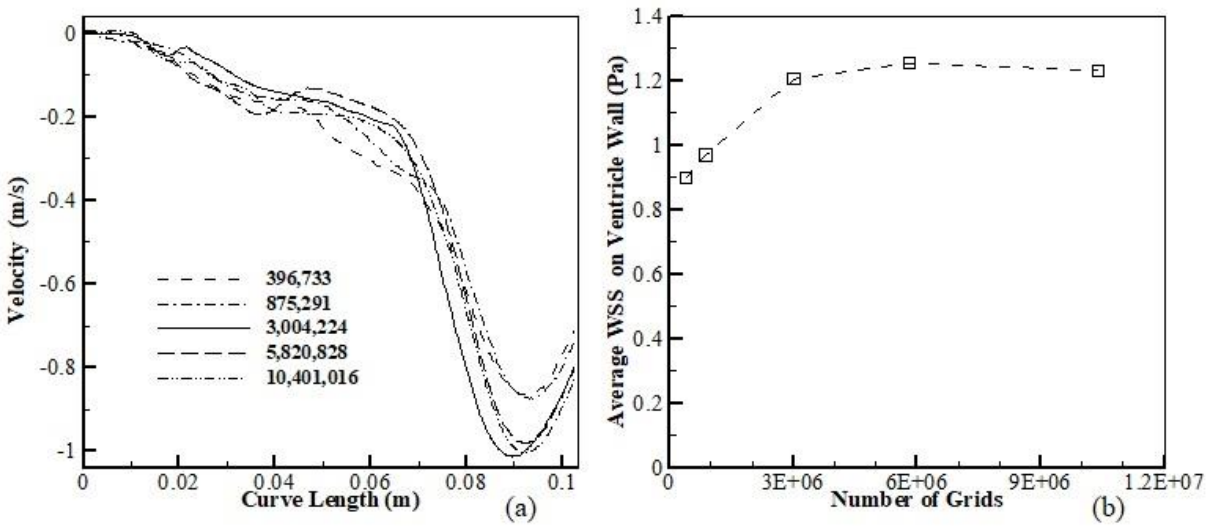

Fig. 2 a) Velocity along the mitral centerline, b) Average WSS vs. grids at t/T = 0.5.

The end-diastolic geometry of the left heart walls was determined on the basis of the geometry given in Chnafa et al. [20]. It has been assumed that the ventricle wall is contracted cylindrically toward a semi-conical shape and the atrium wall is contracted spherically. This assumption is not complete, but it has been assumed by reviewing magnetic resonance images considered in published works. According to Schenkel et al. [22], the valves cannot be segmented as precisely as the geometry of the ventricle endocardium, and most magnetic resonance imaging measurements lack adequate resolution in the valve areas to segment enough base points for a description of the valve position and shape. The limited resolution of medical imaging tools does not allow routinely imagining of the valve through its motion [23]. Consequently, in this model for simplicity, the shapes of the MV and aortic valve (AV) orifices were set so that they were both circular. The MV area to assure the filling of the ventricle with a minimum pressure gradient between LA and LV to prevent intraventricular negative pressure varies between 4 and 6 cm^2 [1]. To consider the MV stenosis the area of AV assumed constant equal to 2 cm^2 but MV areas have been varied from 2 to 6 cm^2 in the cases studied.

The computational model of the left heart as a flow domain that starts from pulmonary veins as pressure inlet, atrium chamber, MV, ventricle chamber, AV, and the initial part of the aorta is constructed. The initial geometry was chosen from the literature. The Initial conditions of zero velocity and pressure were selected. To avoid initial effects the first three cycles have been neglected. The boundary condition includes no-slip moving walls, inlet (pulmonary veins) and outlet (aortic orifice). Constant pressure of 5 mmHg is set for inlet and different pressures of 120 and 80 mmHg is set for outlet during systole and diastole, respectively.

The blood pressure during early diastole is insufficient to drive out the wall of the LV, and deformation of the LV wall during an early diastolic phase is originated by relaxation of the myocardium contracted during a systolic phase [24]. E/A ratio is a marker of the left ventricle function which represents the relationship between the peak velocity of blood flow during early diastole (E wave) and late diastole (A wave). In the present study, deformation of the wall of the LA and LV are set as input boundary conditions so that the flows which can be considered as volume derivative were obtained. Blood flow through MV are given and compared with the results of Chnafa et al. [20] which reported E/A=4.8 in Fig. 3. One of the diastolic dysfunction symptoms is smaller E/A ratio. To consider this phenomenon, in one case (A_{mitral}=2 cm^2), the flow during E wave versus A wave has been modified from 4.8 to 1.

A plane in the MV opening is considered as an interface between atrium and ventricle chambers. The normal vector of this plane is aligned to the apex of the ventricle. In the present study, opening and closing of the MV and AV were assumed as instantaneous events, and during systole phase MV is close and AV is open, while during diastole phase MV is open, and AV is close. The opening and closing valve time are negligible compared to the heart cycle duration [20], which justifies this assumption for simulation of heart whole cycle in addition to the assumed conical shape of the MV to compare its different effective area effect on LV flow pattern.

The blood pressure during the early diastole is not high enough to push out the wall of the LV, but deformation of the LV wall during diastolic phase by relaxation of the myocardium could draw blood from LA to LV [24]. The needed power in E wave is applied by ventricle myocardium relax-

Table 1 Properties of cases with different MV areas

Case	A6	A5	A4	A3	A2
MV area (cm^2)	6	5	4	3	2
E/A ratio	4.8	4.8	4.8	4.8	4.8
EF (%)	48	48	48	48	48
Beats/min	60	60	60	60	60

Table 2 Properties of different cases with MV area of 2 cm^2

Case	A2	EF40	EF24	HR120	EA1
MV area (cm^2)	2	2	2	2	2
E/A ratio	4.8	4.8	4.8	4.8	1
EF (%)	48	40	24	24	48
Beats/min	60	60	60	120	60

ation while in A wave is applied by atrium contraction. The power required for stenosed MV during E wave is higher than other cases which heart may not afford. This suction is limited by the force and energy that could be applied by the myocardium wall. To compensate for that, one approach could be passing less flow through MV because it cannot provide the energy needed for pumping. By reducing the blood flow to compensate for anemia, the heart will have to beat at a faster rate. As a result, less work is done in each pulse and the heart goes through more cycles. To account for what may be due to the heart's inability to back to its relaxation volume in the reduced area of the MV, first, it has been assumed that the flow through the MV would be reduced. As another option, it has been considered that although the flow rate of the heart was reduced in one cycle, it would take a shorter time to compensate for the deficit and to double the HR. The other approach may be reduction of E/A ratio which more flow enters the ventricle by LA contraction. If the LA inflow is the same as normal case, this means that during E wave, LA volume should be increased to compensate for the lower flow rate. This means that three symptoms could be present in this disease: Firstly, lower E/A ratio, secondly, enlarged LA, and finally, atrial fibrillation [25].

In the present work, nine different cases have been studied. These cases are summarized in Tables 1 and 2. In cases A6 to A2 only MV areas are decreased from 6 to 2 cm^2. In EF40 and EF24 cases, the MV area is 2 cm^2 and EF ratio is decreased to 40 and 24, respectively. The case HR120 is similar to EF24 with increased HR from 60 to 120 beats per minute. The last case EA1 is similar to A2 but as shown in Fig. 3 the MV flow pattern has been modified by assuming E/A=1.

3- Results and Discussion

The effect of MV stenosis on ventricular hemodynamic of blood flow was studied. The LA and LV geometries were extracted from the literature, and wall motions were inserted in a way to obtain the reported valve flows. While the focus of this work was not on the MV structure and its leaflet behavior during the short time between systole and diastole, a simplified MV conical shape and instantaneous opening were employed. To compare the effect of MV area, five cases with

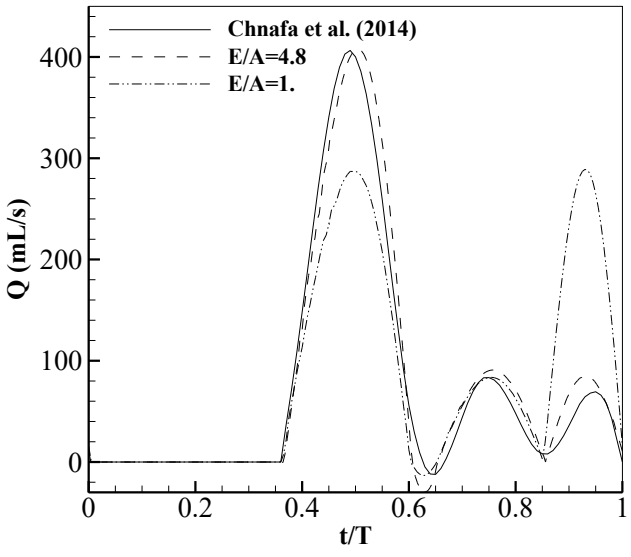

Fig. 3 MV flow in a heart cycle for E/A= 4.8 and 1 and comparison with Chnafa et al. [20] (E/A=4.8)

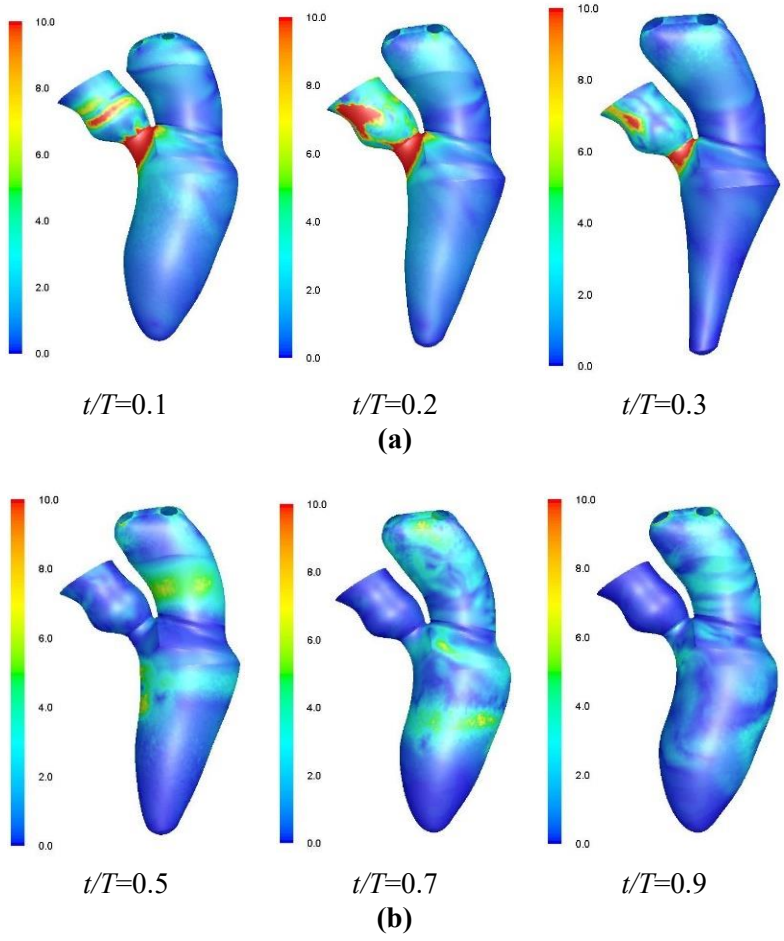

Fig. 4 Wall shear stress distribution at for A5 at different times in a) systole and b) diastole

the same atrium and ventricle geometry and different MV areas ranging from 6 to 2 cm^2 were considered. Heart flow rates through MV in a heart cycle were obtained numerically then compared with the results of Chnafa et al. [20]. The flow is in overall good agreement in both values and trends as shown in Fig. 3.

Fig. 4 depicts the wall shear stress for MV area of 5 cm^2. The first row is during systole phase when MV is close and AV is open, while second row is during diastole phase when MV is open, and AV is close. The boundary motion is shown by ventricle contraction in the first one-third of the cycle (t/T=0.1, 0.2, 0.3) and ventricle dilation in the next two-third of the cycle (t/T=0.5, 0.7, 0.9). Because of flow exit from AV in systole the maximum shear is seen in this area. In diastole the magnitude of wall shear stress is decreased and high shear zones are observed by local phenomena. The wall shear stress contours for the studied cases at t/T=0.5 are depicted in Fig. 5. Increased MS leads to increased wall shear stress. Also, decreased EF and HR causes decreased wall shear stress. The justification for these results is possible by studying the flow field.

Velocity vectors and magnitude contours for all the simulated cases are shown in Figs. 6 and 7 for t/T=0.5 and 0.6, respectively. For all cases, one jet is flowing through the valve and propagating toward the ventricle's apex. For smaller MV areas the maximum velocities occur in the center of the jet while for greater MV areas similar to results given by Vellguth et al. [6], the maximum velocities are located at the end of the jet near its lips because of the pulling the flow with ventricle wall expansion during early diastole.

Based on Fig. 5, a delayed dissipation of early diastole jet occurs in smaller MVs. According to higher limits of the contours' legend, increasing of velocity magnitude changes from 0.81 m/s to 2.62 m/s at t/T=0.5 and from 0.95 to 2.75 m/s at t/T=0.6 for cases from A6 to A2, respectively. Decreased EF, decreased HR and decreased E/A ratio lead to decreased velocity magnitude during early diastole.

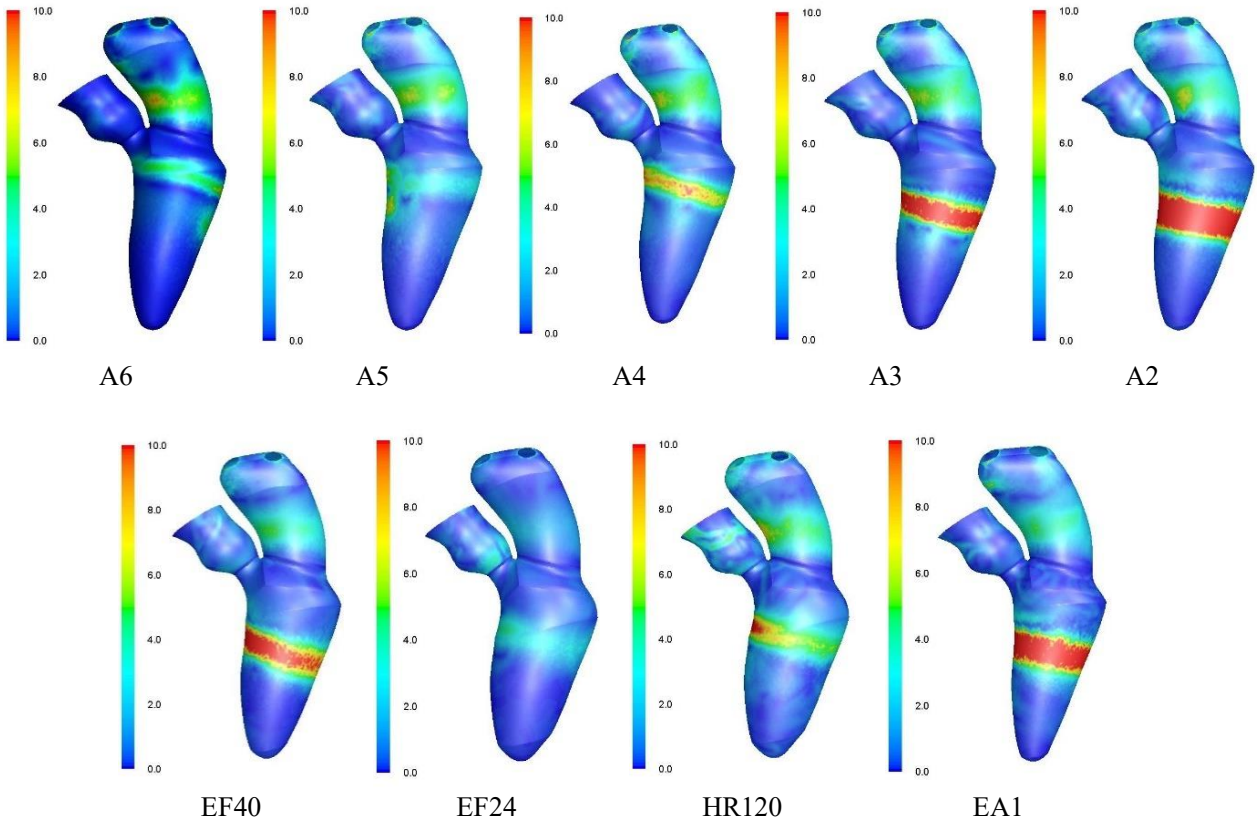

Fig. 5 Wall shear stress distribution at t/T=0.5

Contours of the static pressure at t/T=0.5 and 0.6 are shown in Figs. 8 and 9, respectively. The pressure in the vortex region is lower than the surrounding pressure which is in accordance with Khalafvand et al., [26]. During the early diastole at t/T=0.5, the static pressure in the atrium is higher than the ventricle, but through time the static pressure in the LV exceeds the LA. Based on the upper and lower limits of pressure in the plane observed at t/T=0.5, the pressure difference in the domain is 600, 650, 1100, 1900, and 4300 Pa for A6 to A2 cases, respectively, which shows the effect of stenosis on pressure difference between ventricle and atrium. At t/T=0.6, the pressure in ventricle is higher than atrium and the pressure difference in the domain is 800, 600, 700, 1000, 2500 Pa for A6 to A2 cases, respectively. Both times shows higher pressure gradient in cases with smaller MV area. To consider the effect of different flows, the pressure gradient at t/T=0.5 is 4300, 2900, and 1050 Pa for EF=48%, 40% and 24%, respectively. At t/T=0.6 they become 2500, 2100, and 500 Pa, respectively. Increasing the HR from 60 to 120 leads to an increase of pressure gradient from 1050 to 4300 Pa at t/T=0.5 and from 500 to 1900 Pa at t/T=0.6. Comparing E/A ratio shows that decreasing it from 4.8 to 1 changes the pressure gradient from 4300 to 2500 Pa at t/T=0.5 and from 2500 to 1400 Pa at t/T=0.6. It can be concluded that the pressure difference increases in decreased MV areas and increased EF, HR and E/A ratio cases. The difference will affect the needed work to pump the blood and will be discussed later.

Variations of the LA and LV volumes during a heart cycle are plotted in Figs. 10(a) and 10(b), respectively. For E/A=4.8 the maximum LA volume occurs at the end of systole while for E/A=1 it occurs during diastole. In addition, its maximum is higher, which means that the LA volume has been increased more than its normal diastole size. During early diastole of LV the rate of volume increase is higher for E/A=4.8 but this increase is smoother for E/A=1.

The rise and reduction in pressure variation are associated to flow acceleration and deceleration [26]. This pressure variation along with myocardium motion determines the power inserted by heart chambers. Three different stages could be defined for the explanation of LV power plot shown in Fig. 11. In the first stage during systole, when MV is close, the ventricle contraction pumps the blood to aorta. In the next stage during the E wave the MV is open and LV relaxation draws the blood from LA. MV area affects the pressure gra-

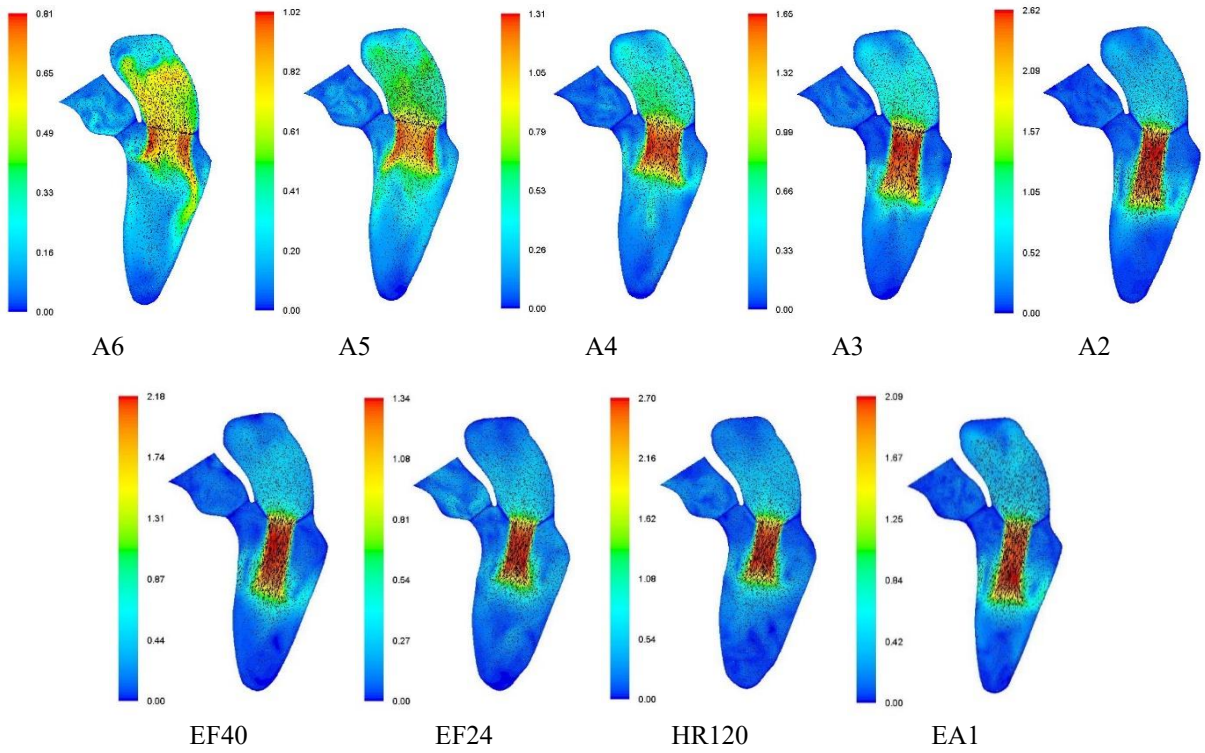

Fig. 6 Velocity magnitude distribution at t/T=0.5

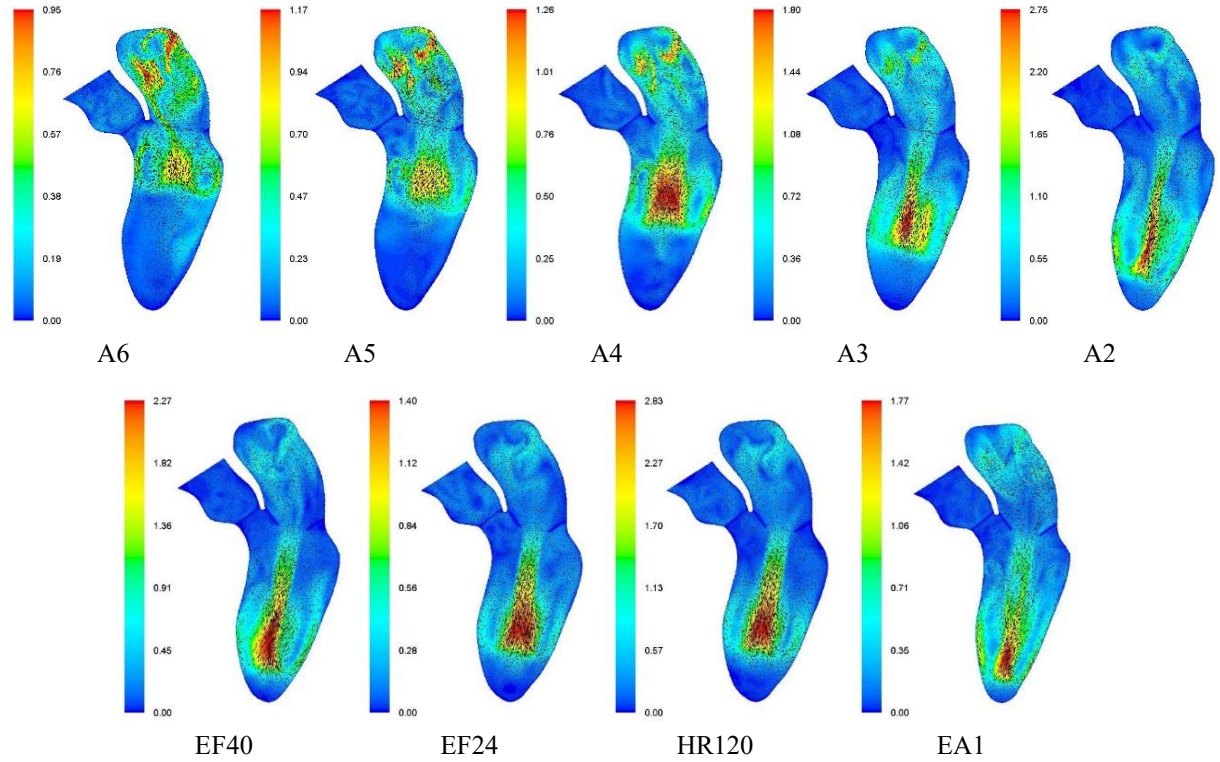

Fig. 7 Velocity magnitude distribution at t/T=0.6

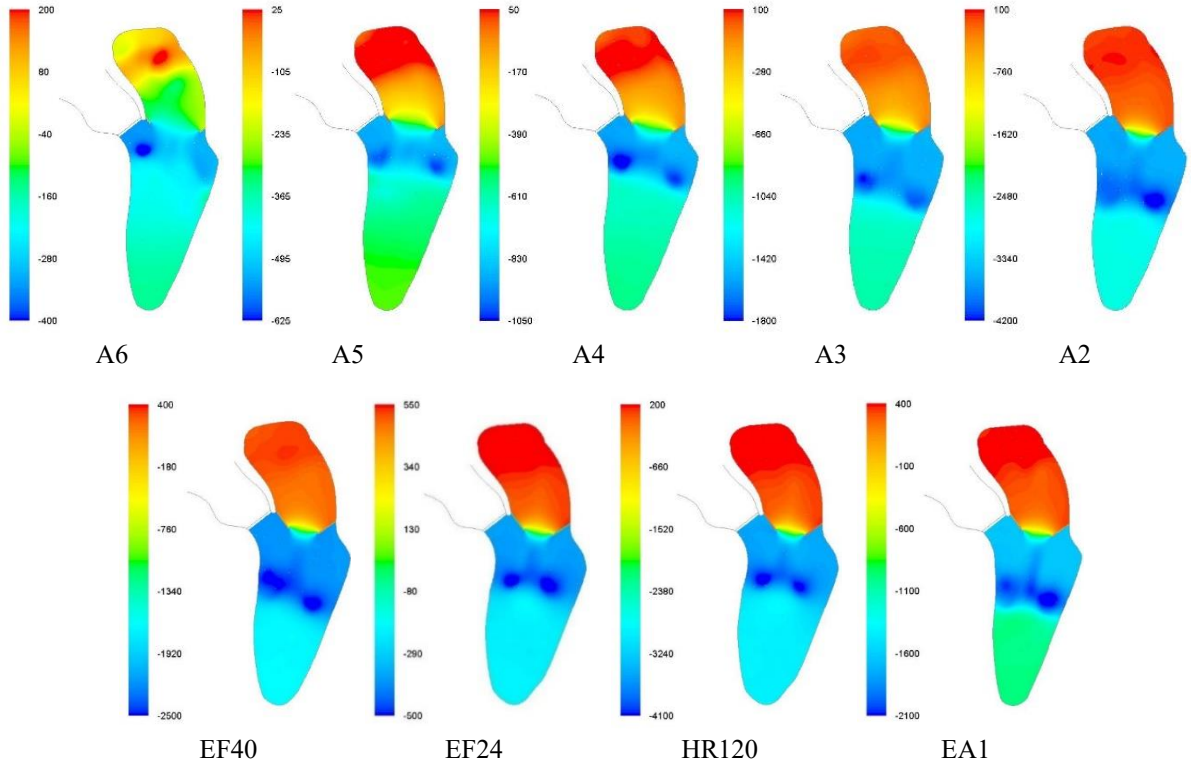

Fig. 8 Static pressure distribution at t/T=0.5

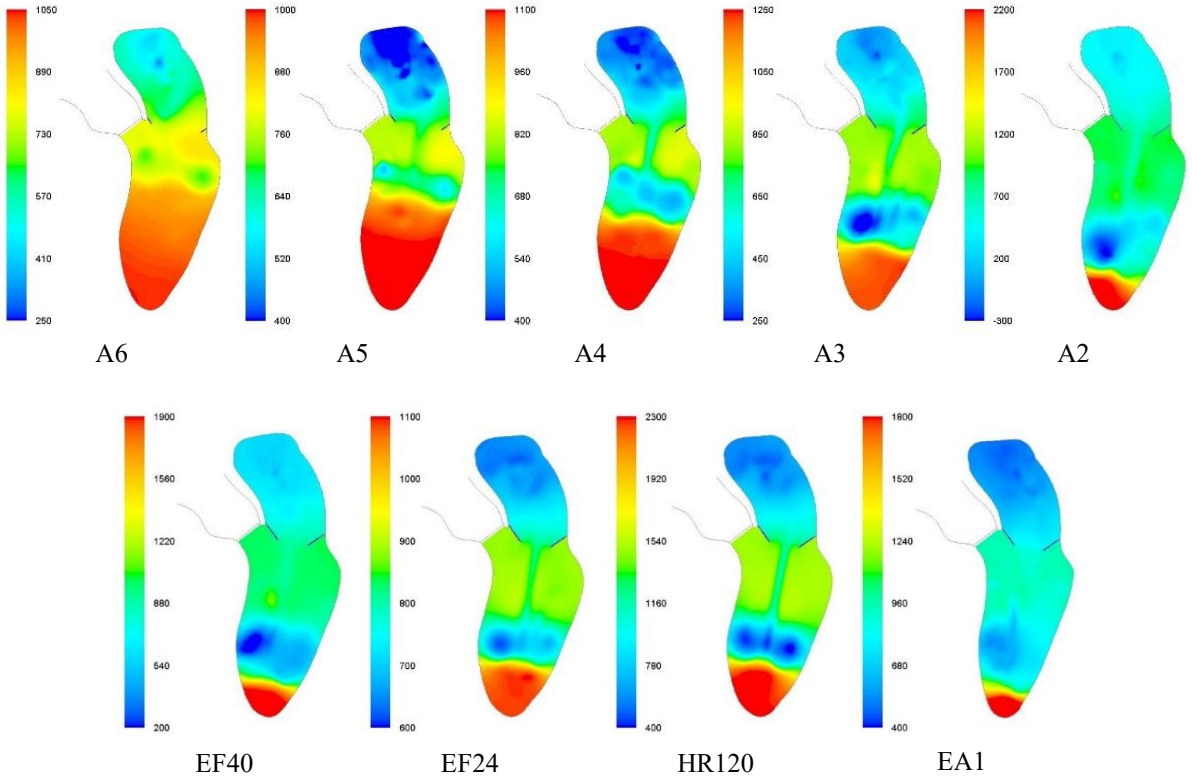

Fig. 9 Static pressure distribution at t/T=0.6

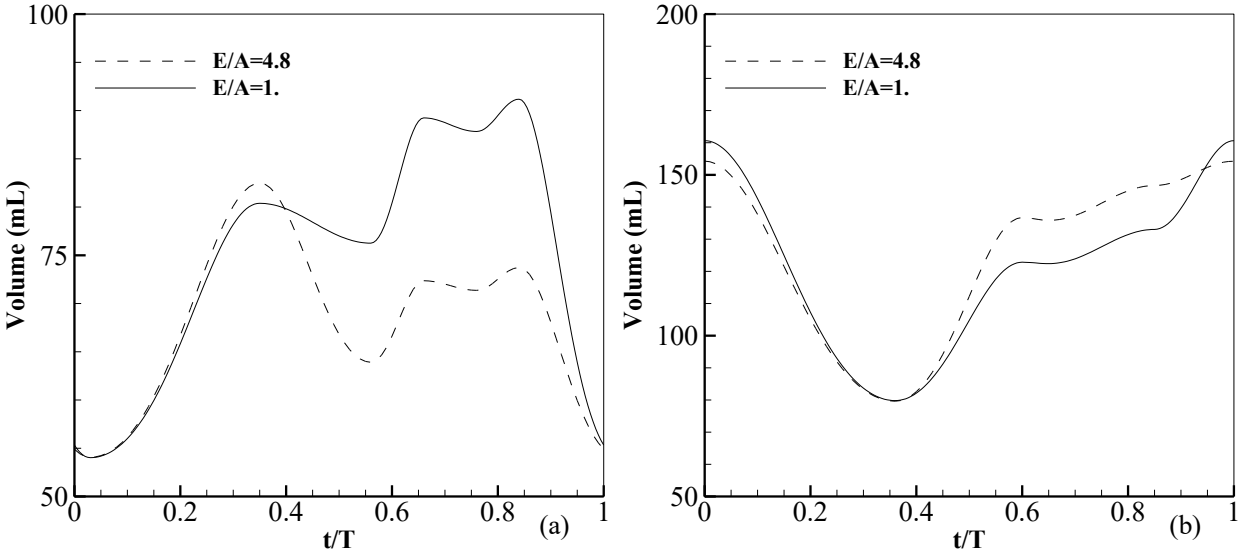

Fig. 10 Heart chambers including a) LA, and b) LV volume during a heart cycle for MV area of 2 cm2

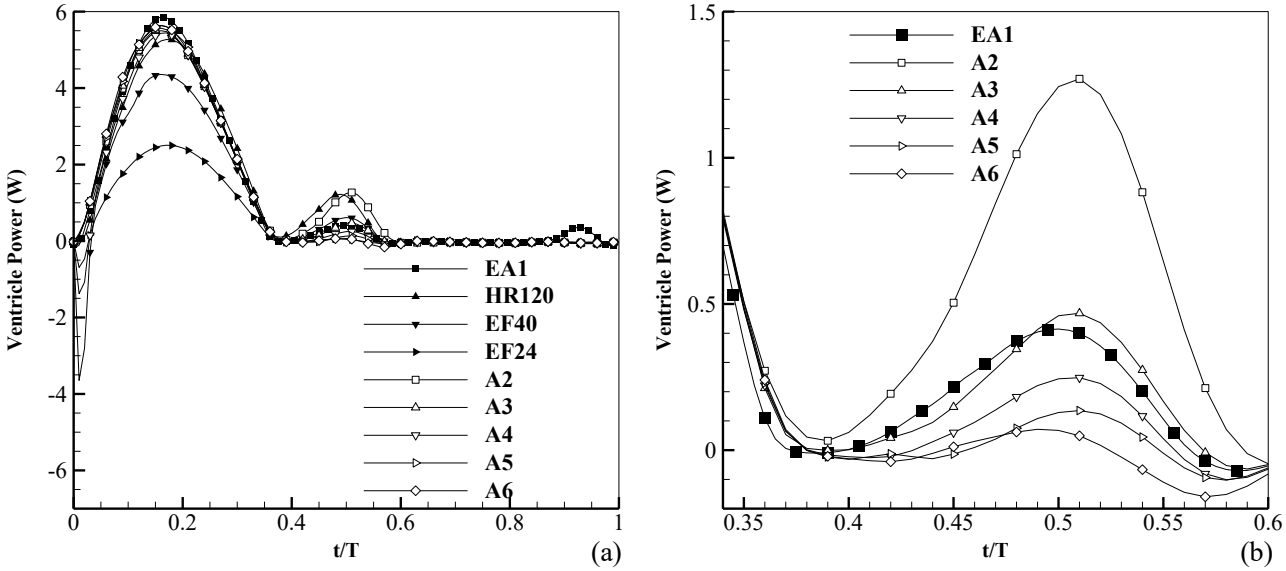

Fig. 11 Ventricle power versus time during a) heart cycle, and b) early diastole

dient between LA and LV significantly, and it is higher for smaller MV areas. The last stage, during the late diastole, is the relaxation phase. Since the flow through MV is decreased the pressure difference is low and needs negligible power by LV myocardium.

Variations of the LV power during heart cycle shows that decreasing MV area increases the maximum myocardium work done during early diastole. The assumed methods for reduction of this work in reduced heart EF ratio decreases the power of systole and early diastole. Increased HR to compensate for the blood flow rate diminishes the effect of decreased EF in heart work reduction, consequently, the power variations of cases A2 and HR120 are similar. On the other hand, modification of E/A ratio to 1 decreases the early diastole work without changing the systolic power. Only a small peak can be seen at the end diastolic region of heart power.

4- Conclusions

The variety of parameters have been studied numerically to find the effect of mitral stenosis and heart compensation mechanism. It was found that decreased area from 6 to 2 cm^2 increases the needed maximum heart power from 0.06 W to 1.28 W in early diastole. Results show that a decrease in the MV area causes a high-pressure gradient between LA and LV. It means that LV should apply a higher force and energy to preserve the blood flow rate in the normal range that could be much greater than that applied by the myocardium of LV wall in a heart with a healthy MV area of 4 to 6 cm^2. Early diastolic power during E wave is applied by ventricular myocardium relaxation. Since LV may not afford such power, heart should be adopted to solve the problem. Two different scenarios have been assumed to compensate for this problem based on the studied symptoms of this disease. The first one was the reduction of EF ratio and an increase in HR that has been shown that couldn't solve the problem. In the early diastole, decreasing the E/A ratio from 4.8 to 1 decreased the maximum ventricle power to one-third so the second option could be a modification of E/A ratio which has shown that it is possible and are in accordance with the symptoms of this disease, including decreased E/A ratio, increased volume of the atrium, and fibrillated atrium.

References

[1] F.F. Faletra, Echocardiography in mitral valve disease, Springer, Milan, 2013.

[2] F. Sotiropoulos, T.B. Le, A. Gilmanov, Fluid mechanics of heart valves and their replacements, Annual Review of Fluid Mechanics 48, (2016) 259-283.

[3] C.W. Baird, G.R. Marx, M. Borisuk, S. Emani, P.J.D. Nido, Review of congenital mitral valve stenosis: analysis, repair techniques and outcomes, Cardiovascular Engineering and Technology, 6 (2015) 167-173.

[4] S.C. Harb, B.P. Griffin, Mitral valve disease: a comprehensive review, Current cardiology reports 19(8) (2017) 73.

[5] J. Liao, I., Vesely, A structural basis for the size-related mechanical properties of mitral valve chordae tendineae, Journal of biomechanics, 36(8) (2003) 1125-1133.

[6] K. Vellguth, J. Brüning, L. Goubergrits, L. Tautz, A. Hennemuth, U. Kertzscher, F. Degener, M. Kelm, S. Sündermann, T. Kuehne, Development of a modeling pipeline for the prediction of hemodynamic outcome after virtual mitral valve repair using image-based CFD, International journal of computer assisted radiology and surgery, 13(11) (2018) 1795-1805.

[7] K.L. Chan, K. Hay, B.K. Lam, Prognostic significance of mitral stenosis indices on outcomes in patients following mitral valve repair for degenerative mitral regurgitation, Journal of the American College of Cardiology, 69 (2017) 1971.

[8] D. Goldstein, A.J. Moskowitz, A.C. Gelijns, G. Ailawadi, M.K. Parides, L.P. Perrault, J.W. Hung, P. Voisine, F. Dagenais, A.M. Gillinov, V. Thourani, Two-year outcomes of surgical treatment of severe ischemic mitral regurgitation, New England Journal of Medicine 374(4) (2016) 344-353.

[9] Y.N. Nguyen, M. Ismail, F. Kabinejadian, E.L.W. Tay, H.L. Leo, Post-operative ventricular flow dynamics following atrioventricular valve surgical and device therapies: A review, Medical engineering & physics, 54 (2018) 1-13.

[10] E. Votta, T.B. Le, M. Stevanella, L. Fusini, E.G. Caiani, A. Redaelli, F. Sotiropoulos, Toward patient-specific simulations of cardiac valves: state-of-the-art and future directions, Journal of biomechanics, 46(2) (2013) 217-228.

[11] S.A. Esfahani, K. Hassani, D.M. Espino, Fluid-structure interaction assessment of blood flow hemodynamics and leaflet stress during mitral regurgitation, Computer methods in biomechanics and biomedical engineering, 22(3) (2019) 288-303.

[12] B. Su, X. Wang, F. Kabinejadian, C. Chin, T.T. Le, J.M. Zhang, Effects of left atrium on intraventricular flow in numerical simulations, Computers in Biology and Medicine, 106 (2019) 46-53.

[13] V. Meschini, F. Viola, R. Verzicco, Modeling mitral valve stenosis: A parametric study on the stenosis severity level. Journal of biomechanics, 84 (2019) 218-226.

[14] V. Meschini, F. Viola, R. Verzicco, Heart rate effects on the ventricular hemodynamics and mitral valve kinematics, Computers & Fluids, 197 (2020) 104359.

[15] B. Su, L. Zhong, X-K. Wang, J-M. Zhang, R.S. Tan, J.C. Allen, S.K. Tan, S. Kim, H.L. Leo, Numerical simulation of patient-specific left ventricular model with both mitral and aortic valves by FSI approach, Computer Methods and Programs in Biomedicine, 113 (2014) 474-482.

[16] H. Kitajima, A.P. Yoganathan, Blood flow-the basics of the discipline. In: Fogel, M.A., (Ed.). Ventricular Function and Blood Flow in Congenital Heart Disease, Blackwell Publishing, (2005) http://doi.org/10.1002/9780470994849.ch3.

[17] J. Smagorinsky, General Circulation Experiments with the Primitive Equations. I. The Basic Experiment, Monthly Weather Review, 91 (1963) 99-164.

[18] Fluent, ANSYS, (2015) Theory guide. Ansys Inc.

[19] R. Mittal, J.H. Seo, V. Vedula, Y.J. Choi, H. Liu, H.H. Huang, ... & R.T. George, Computational modeling of cardiac hemodynamics: Current status and future outlook, J. Comput. Phys., 305 (2016) 1065-1082.

[20] C. Chnafa, S. Mendez, F. Nicoud, Image-based large-eddy simulation in a realistic left heart, Comput. Fluids,

94 (2014) 173-187.

[21] R. Samian, M. Saidi, Investigation of left heart flow using a numerical correlation to model heart wall motion, Journal of Biomechanics, 93 (2019) 77-85.

[22] T. Schenkel, M. Malve, M. Reik, M. Markl, B. Jung, H. Oertel, MRI-based CFD analysis of flow in a human left ventricle: methodology and application to a healthy heart, Annals of biomedical engineering, 37(3) (2009) 503-515.

[23] C. Celotto, L. Zovatto, D. Collia, G. Pedrizzetti, Influence of mitral valve elasticity on flow development in the left ventricle, European Journal of Mechanics-B/Fluids, 75 (2019) 110-118.

[24] M. Nakamura, S. Wada, T. Mikami, A. Kitabatake, T. Karino, Computational study on the evolution of an intraventricular vortical flow during early diastole for the interpretation of color M-mode Doppler echocardiograms, Biomechanics and Modeling in Mechanobiology 2(2) (2003) 59-72.

[25] K.H. Olesen, The natural history of 271 patients with mitral stenosis under medical treatment, British heart journal, 24(3) (1962) 349.

[26] S.S. Khalafvand, E.Y.K. Ng, L. Zhong, T.K. Hung, Fluid-dynamics modeling of the human left ventricle with dynamic mesh for normal and myocardial infarction: Preliminary study, Computers in Biology and Medicine 42 (2012) 863-870.

HOW TO CITE THIS ARTICLE

M. Saidi , R. Samian , Numerical investigation of cardiac function parameters in left heart hemodynamics with stenosed mitral. AUT J. Mech Eng., 5(3) (2021) 465-476.

DOI: 10.22060/ajme.2020.18606.5906